JACS
JOURNAL OF THE AMERICAN CHEMICAL SOCIETY
Article
pubs.acs.org/JACS

The Novel Chemical Mechanism of the Twister Ribozyme

Timothy J. Wilson,[†] Yijin Liu,[†] Christof Domnick,[‡] Stephanie Kath-Schorr,[‡] and David M. J. Lilley*[,†]

[†]Cancer Research UK Nucleic Acid Structure Research Group, MSI/WTB Complex, The University of Dundee, Dow Street, Dundee DD1 5EH, U.K.

[‡]Life and Medical Sciences Institute, University of Bonn, Gerhard-Domagk-Strasse 1, 53121 Bonn, Germany

Supporting Information

ABSTRACT: We describe the multifactorial origins of catalysis by the twister ribozyme. We provide evidence that the adenine immediately 3′ to the scissile phosphate (A1) acts as a general acid. Substitution of ring nitrogen atoms indicates that very unusually the N3 of A1 is the proton donor to the oxyanion leaving group. A1 is accommodated in a specific binding pocket that raises its pK_a toward neutrality, juxtaposes its N3 with the O5′ to be protonated, and helps create the in-line trajectory required for nucleophilic attack. A1 performs general acid catalysis while G33 acts as a general base. A 100-fold stereospecific phosphorothioate effect at the scissile phosphate is consistent with a significant stabilization of the transition state by the ribozyme, and functional group substitution at G33 indicates that its exocyclic N2 interacts directly with the scissile phosphate. A model of the ribozyme active site is proposed that accommodates these catalytic strategies.

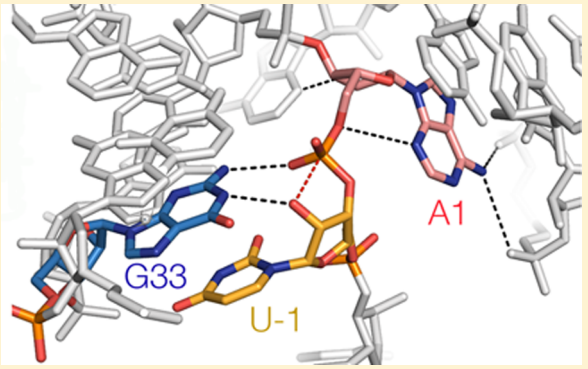

INTRODUCTION

RNA catalysts (ribozymes) are ubiquitous and RNA catalysis is used to perform some of the cell's most important reactions.[1,2] The nucleolytic ribozymes are an ever-growing group of ribozymes that carry out site-specific cleavage and ligation reactions in RNA. They serve to process replication intermediates and control gene expression. Some members of this class are widespread in the genomes of living species from bacteria to humans;[3,4] in many cases they appear to be functional, yet their role is presently unclear.

The nucleolytic ribozymes accelerate their cleavage reactions by at least a million fold. The catalytic mechanisms by which this is achieved have been the subject of considerable investigation and debate, yet remain incompletely understood. The chemical mechanism of the cleavage reaction is shown in Figure 1A. Four aspects of the reaction could be rate limiting, and are therefore candidates for catalytic intervention. These processes are

1. Achievement of an in-line trajectory such that the O2′ nucleophile, the phosphorus of the scissile phosphate and the O5′ leaving group are colinear.
2. Stabilization of the phosphorane transition state structurally and/or electrostatically.
3. Activation of the O2′ nucleophile. A hydroxyl is a poor nucleophile, but removal of the proton by a general base leaves a much more potent alkoxide nucleophile.
4. Facilitation of the departure of the leaving group. Protonation of the O5′ oxyanion by a general acid converts it into a superior leaving group.

The in-line trajectory is necessary but not sufficient for effective catalysis as it increases the rate of reaction by no more than 2 orders of magnitude.[5] Each of the nucleolytic ribozymes must adopt a folded structure that achieves an in-line trajectory and utilize some combination of the other three processes to further enhance reactivity. Coordinated processes 3 and 4 constitute general acid−base catalysis. In general terms this class of ribozyme uses general acid−base catalysis, often mediated by nucleobases, but no two ribozymes use identical catalytic strategies and each newly characterized ribozyme has expanded our knowledge of the inherent possibilities of RNA catalysis.

Breaker and colleagues have identified four new nucleolytic ribozymes in the last two years.[6,7] The first of these was called twister,[6] for which 2690 examples have been found distributed in the genomes of bacteria, fungi, plants and animals including vertebrates. Although their functions are not known, their locations and the high conservation of active sequences suggests a role in genetic control. We have solved the structure of the twister ribozyme by X-ray crystallography and investigated its chemical mechanism.[8] The global fold is based on a reversed double-pseudoknot structure that brings together the highly conserved nucleotides in loops L1 and L4 to form the active site (Figure 1B, C). G33 (the new systematic numbering system for the twister ribozyme is explained in Figure S1 and a key aligning the three crystal structures to the new system is provided in Table S1) was observed to donate a

Received: November 10, 2015
Published: May 6, 2016

DOI: 10.1021/jacs.5b11791
J. Am. Chem. Soc. 2016, 138, 6151−6162

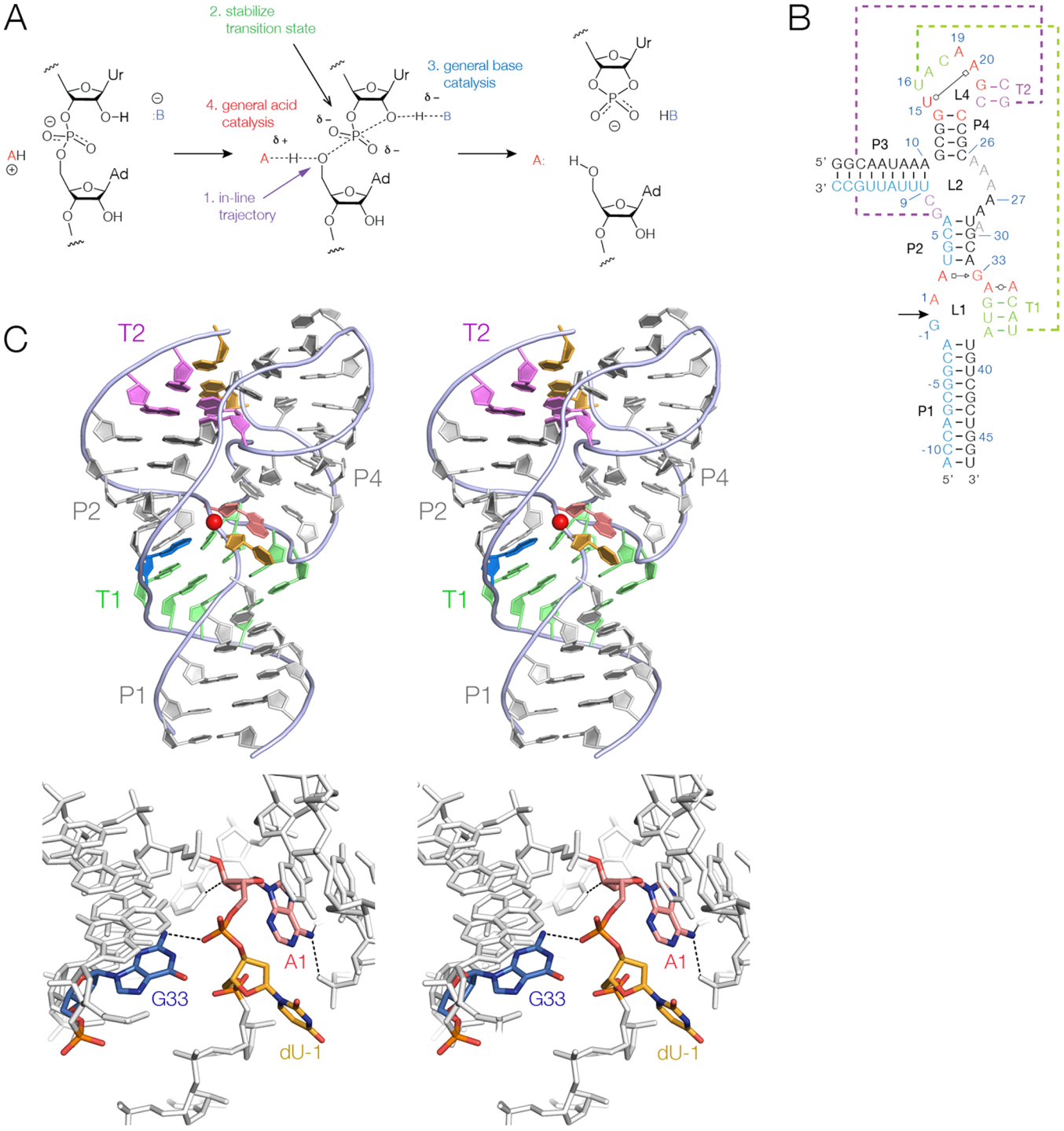

Figure 1. Twister ribozyme. (A) The chemical mechanism and potential sources of catalysis in the nucleolytic ribozymes. The cleavage reaction is initiated by attack of the O2′ nucleophile on the phosphorus, and proceeds via a phosphorane species (center) that will be close to the transition state. Four catalytic strategies are highlighted. (B) The sequence and nomenclature of the twister ribozyme. The two-piece ES2 ribozyme used in the cleavage experiments is shown, with the substrate strand in blue. Cleavage occurs at the arrowed position, and the two long-range tertiary interactions T1 and T2 are indicated. Highly conserved nucleotides are written in red. A new nucleotide numbering system is shown that begins at the A 3′ to the cleavage site. This continues sequentially, through P2, the first basepair of helix P3, P4 and loop L4 that makes the tertiary interactions. Poorly conserved nucleotides in and around loop L2 (colored gray) are not included in the numbering. (C) The crystal structure of the twister ribozyme from *Oryza sativa*,[8] shown in parallel-eye stereoscopic view. A deoxyuridine was incorporated at position −1 so that the ribozyme was inactive. Upper: A view of the complete ribozyme structure. P1, T1, P2 and T2 plus P3 if present form a continuous helical stack. The scissile phosphate is indicated by the red sphere, and the nucleotides dU-1, A1 and G33 are colored orange, red and blue, respectively. The tertiary interactions T1 and T2 are colored green and purple. The *O. sativa* ribozyme lacks a P3 helix, but what would be the first basepair (C9-G10) is colored orange. The intervening nucleotides are not shown. Lower: A closer view of the catalytic center. dU-1 is far from the required in-line orientation. G33 donates a hydrogen bond from its N2 to the *pro*R nonbridging oxygen of the scissile phosphate. A1 has a 2′-*endo* sugar pucker and is held in the *syn* conformation by hydrogen bonds donated by the N6 of A1 to nonbridging oxygens of the phosphates of C16 and C17.

DOI: 10.1021/jacs.5b11791
J. Am. Chem. Soc. 2016, 138, 6151−6162

Table 1. Observed Cleavage Rates (min^{-1}) for the Twister Ribozyme and Variants, Using the Two Piece ES2 Ribozyme[a]

		pH 5.5			pH 7.0			pH 8.5			pK_a	
position 1	ribozyme	k_{obs}	±	fold	k_{obs}	±	fold	k_{obs}	±	fold	nucl	obs
A[b]	ES2	0.35	0.02		2.45	0.04		3.5	0.5		3.64	6.9
G[b]	ES2	0.00017	0.00008	2100	0.00024	0.00007	10000	0.0019	0.0003	1900		
A N7C	ES2	0.10	0.02	3.5	1.37	0.04	1.8	>8			5.2	
A N7C	A20G	0.018	0.002	2.1	0.28	0.01	0.8	2.2	0.2	0.20		8.5
A[b]	A20G	0.038	0.009	9.2	0.23	0.02	11	0.43	0.02	8.1		7.0
A N3C O2′H	ES2	–			0.00003	0.00001	32000	0.00004	0.000005			
A O2′H	ES2	–			0.97	0.04	2.5	–				
A N1C	A19U	0.06	0.01	0.15	1.1	0.3	0.05	7.7	1.0	0.01	4.7	
A	A19U	0.0092	0.0005	38	0.059	0.004	42	0.10	0.01	35		6.9

[a]All rates were measured in the presence of 10 mM $MgCl_2$. Most rates were measured at three different pH values, pH = 5.5, 7.0, and 8.5. The error (±) is twice the standard deviation. The final two columns show the pK_a values of the nucleotide at the 1 position as the free nucleotide (nucl) and the observed value measured in ribozyme cleavage reactions (obs). The fold changes in rate are calculated for the A1 variants as a ratio of that measured for the variant that differs only in that position; values >1 reflect fold reduction in rate. [b]Data taken from our previous study.[8]

hydrogen bond from its N2 to the *pro*R nonbridging oxygen of the scissile phosphate (Figure 1C), suggesting a possible role in stabilization of the transition state (process 2). The rate of the cleavage reaction exhibits a bell-shaped dependence upon pH corresponding to two ionizations with apparent pK_a values of $pK_{a,1}$ = 6.9 and $pK_{a,2}$ = 9.5, consistent with a concerted general acid−base catalytic mechanism (processes 3 and 4). Substitution experiments demonstrated that G33 was responsible for the higher pK_a value but the origin of the lower pK_a value remained unidentified. The structure does not have the required in-line geometry at the scissile phosphate, because the uridine 5′ to the scissile phosphate has become hydrogen bonded to a guanine in a symmetry-related molecule within the crystal. However, we showed that a simple unhindered rotation of U-1 so that its base is stacked with G33 would bring its O2′ in-line with the phosphate (process 1) and position G33 to act as a general base (process 3). Recent molecular dynamics solution simulations support this positioning of G33.[9] Thus, G33 may have two functions, acting in a manner analogous to G8 and G638 in the hairpin[10−12] and VS ribozymes, respectively.[13−15]

This leaves the question of what contributes the lower pK_a in the reaction rate pH dependence, the probable general acid that will protonate the oxyanion leaving group (process 4). Two other laboratories[16,17] subsequently solved structures of different forms of the twister ribozyme. The global folds are identical but the position of U-1 within the active site varies markedly. Unfortunately neither structure helps to identify a general acid; however A34[16] and Mg^{2+}[17] were identified as possible sources of transition state stabilization (process 2). The structure of Ren et al.[17] has a near in-line conformation; however, as we shall argue below, there is considerable doubt that it represents a catalytically active structure.

In this work we provide evidence that the twister ribozyme uses all four catalytic strategies to accelerate its cleavage reaction. We investigate possible contributions to transition state stabilization using the previously reported phosphorothioate effect,[6,18] and confirm the importance of the hydrogen bond between G33 and the scissile phosphate. We furthermore identify the adenine 3′ to the scissile phosphate (A1) as the general acid, and demonstrate that, most unusually, it acts through the highly acidic N3 nitrogen. We discuss the structural features of the twister ribozyme that enable its novel catalytic mechanism.

RESULTS

A1 Is a Possible Second Catalytic Nucleobase. In our previous mechanistic studies we concluded that the bell-shaped dependence of the cleavage reaction of the twister ribozyme upon pH is best explained by a concerted general acid−base catalytic mechanism, with the higher apparent pK_a value of 9.5 resulting from the ionization of G33.[8] The lower apparent pK_a value of 6.9 is most likely due to the titration of an adenine or cytosine. Of the highly conserved nucleotides, only A1 and A20 are close enough to the scissile phosphate that they might participate in proton transfer (Figure 1C; Figure S2). However, the cleavage rate of an A20G variant ribozyme was only lowered 10-fold and the pH dependence of the reaction was essentially unchanged.[8] These data are not consistent with A20 acting as general acid or base.

In contrast, the A1G ribozyme investigated previously[8] exhibited a 10^4-fold reduction in activity at pH 7.0, with some restoration of cleavage rate at high pH (Table 1). This may indicate that A1 participates in catalysis but it is possible that the very low levels of activity of this substituted ribozyme could arise from misfolding due to the loss of the hydrogen bonds donated by the N6 of A1 (Figure 1C). Recently, the importance of these hydrogen bonds was again demonstrated by the marked reduction in activity due to a 2-aminopurine substitution at position 1 and the partial recovery in activity resulting from a diaminopurine substitution.[18] These authors also showed that the loss of both the N1 and N3 ring nitrogen atoms led to a significant loss of activity, which may be consistent with participation in catalysis although the possibility of structural perturbation was not explored. However, they also reported a pK_a for A1 of 5.2 measured by NMR. This value is not unusual for an adenine nucleobase in a structured RNA[19] and well below the lower apparent pK_a value of 6.9 for the active ribozyme. While it is of some interest to measure the pK_a by a technique like NMR, it is much more valuable to measure the apparent pK_a from the reaction kinetics, because this tells us about the state of the reactants during the reaction progress. This is the value that is relevant to the kinetic processes under study. Thus, the existing data do not eliminate the possibility of A1 participating in catalysis, but neither do they strongly support it. Consequently, we sought to introduce less perturbing A1 substitutions and characterize their pH dependence to investigate further the role of A1 in catalysis.

A1 N7C Substitution Alters the pH Dependence of Catalytic Activity. Examination of the crystal structure

DOI: 10.1021/jacs.5b11791
J. Am. Chem. Soc. 2016, 138, 6151−6162

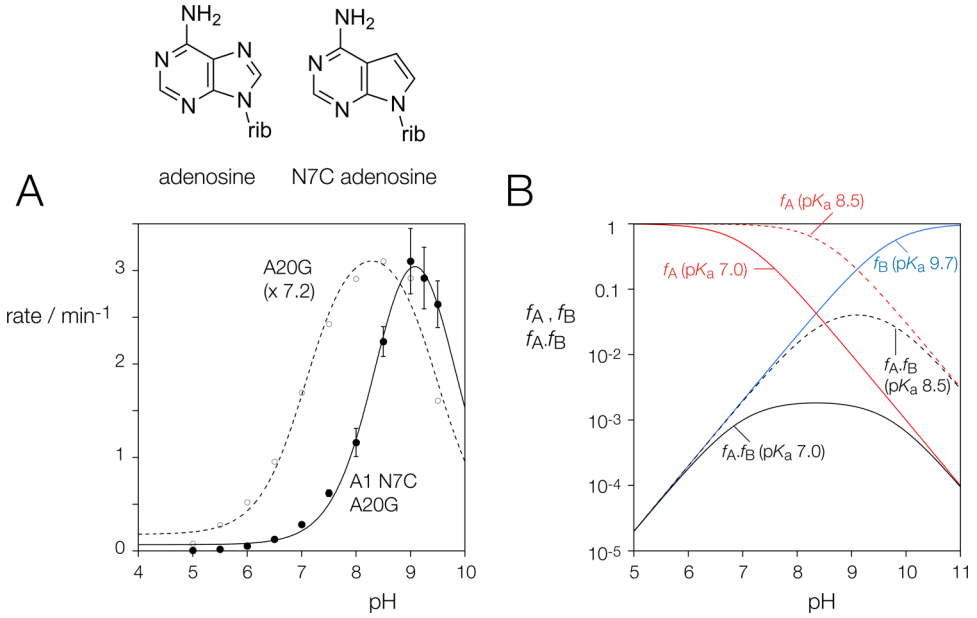

Figure 2. pH dependence of the twister ribozyme on N7C modification of A1. Scheme (top) shows the chemical structure of adenosine and N7C adenosine, which differ by the substitution of N7 by CH. (A) The experimental pH dependence of cleavage rate of the twister ribozyme with A1 N7C and A20G substitutions (unbroken line, filled symbols). These data were fitted to a two-ionization model (eqs 1−3), yielding apparent pK_a values of p$K_{a,1}$ = 8.5 ± 0.1 and p$K_{a,2}$ = 9.7 ± 0.1. The corresponding profile for the single A20G substituted ribozyme is also shown (broken line, open symbols). Note that the A1 N7C, A20G ribozyme has a pH maximum that is shifted to higher pH, and has a maximum that is an order of magnitude faster, compared to the A20G ribozyme. The latter has been scaled by a factor of 7.2 in this plot for ease of comparison. These data are plotted on a logarithmic scale in Figure S3. (B) Simulated pH dependence to show the effect of raising the pK_a of the general acid. The colored lines show the fraction of protonated general acid (f_a, red) and unprotonated general base (f_b, blue) for pK_a values of 7.0 and 8.5 for the general acid (corresponding to apparent values for adenine and N7C adenine in the twister ribozyme), and 9.7 for the general base. The black lines show plots of the product $f_a \times f_b$, representing the fraction of active catalyst; this should reflect the observed pH dependence of the cleavage rate. These curves are bell-shaped, with maxima at 8.35 (for the general acid pK_a = 7.0) and 9.1 (for the general acid pK_a = 8.5). Note that the plots of f_a and f_b intersect at a higher value when the general acid pK_a = 8.5, so that $f_a \times f_b$ is bigger and thus the expected rate will be faster for the N7C adenine substitution.

suggested that substitution of the nucleobase of A1 with 7-deaza-adenine was unlikely to perturb significantly the structure of the ribozyme. The atomic substitution of N7 by a CH (A1 N7C) increases the microscopic pK_a of the N1 and N3 ring nitrogen atoms,[20,21] and if one of these participates in general acid−base catalysis there should be a corresponding change in the pH dependence of the cleavage reaction. We therefore introduced this modified nucleobase at position 1 of the substrate strand of the bimolecular ES2 twister ribozyme used for mechanistic studies (Figure 1B).

It is noteworthy that the ES2 ribozyme cleaves the A1 N7C substrate significantly more rapidly than the natural substrate at high pH (Table 1). The rate is too fast to measure by manual methods so we used a ribozyme with an additional A20G substitution to characterize the pH dependence of the cleavage reaction. The latter modification reduces the cleavage rate of an A1 substrate 10-fold while having no effect on the pH-dependence of the reaction.[8] Cleavage of the A1 N7C substrate by the A20G ribozyme resulted in an apparent p$K_{a,1}$ = 8.5 ± 0.1 (Figure 2A; Figure S3) whereas the A20G ribozyme has an apparent p$K_{a,1}$ = 7.0 ± 0.1 when cleaving an unsubstituted substrate strand.[8] The increase in p$K_{a,1}$ on substitution by A1 N7C is identical, within experimental error, to the difference in the macroscopic acidity constants between adenosine (pK_a = 3.64) and N7C-adenosine (pK_a = 5.2).[20,21] The shift in apparent pK_a demonstrates that A1, in combination with G33, is responsible for the pH dependence of the reaction.

Assuming a catalytic mechanism employing general acid base catalysis, the observed rate of cleavage (k_{obs}) can be considered as the product of k_{int}, the intrinsic rate of cleavage by the ribozyme in the required state of protonation, and $f_a \times f_b$, the fraction of ribozymes in the appropriate protonation state (i.e., a protonated acid with fraction f_a and a deprotonated base with fraction f_b).[22] Thus

$$k_{obs} = k_{int} \times f_a \times f_b \quad (1)$$

where

$$f_a = \left(1 + 10^{pK_a^B - pH}\right) \Big/ \left(1 + 10^{pK_a^B - pH} + 10^{pK_a^B - pK_a^A} + 10^{pH - pK_a^A}\right) \quad (2)$$

$$f_b = \left(1 + 10^{pH - pK_a^A}\right) \Big/ \left(1 + 10^{pK_a^B - pH} + 10^{pK_a^B - pK_a^A} + 10^{pH - pK_a^A}\right) \quad (3)$$

$f_a \times f_b$ is pH dependent and gives rise to the bell-shaped pH dependence of cleavage rate. A1 N7C substitution is predicted to give a 20-fold increase in the maximum value of $f_a \times f_b$ (Figure 2B). The observed increase is lower due to the decreased intrinsic reactivity of the ribozyme since 7-deaza-adenine is a weaker acid than adenine. The intrinsic reactivity is limited by the rate of proton transfer of the weaker of the acid and the base participating in the reaction and in this case the acid is weaker. The Brønsted equation relates the rate to the pK_a of the acid

$$\log k = A - \alpha pK_a \quad (4)$$

where α is the extent of proton transfer in the transition state, which is typically ~0.5 for phosphodiester transfer reac-

DOI: 10.1021/jacs.5b11791
J. Am. Chem. Soc. 2016, 138, 6151−6162

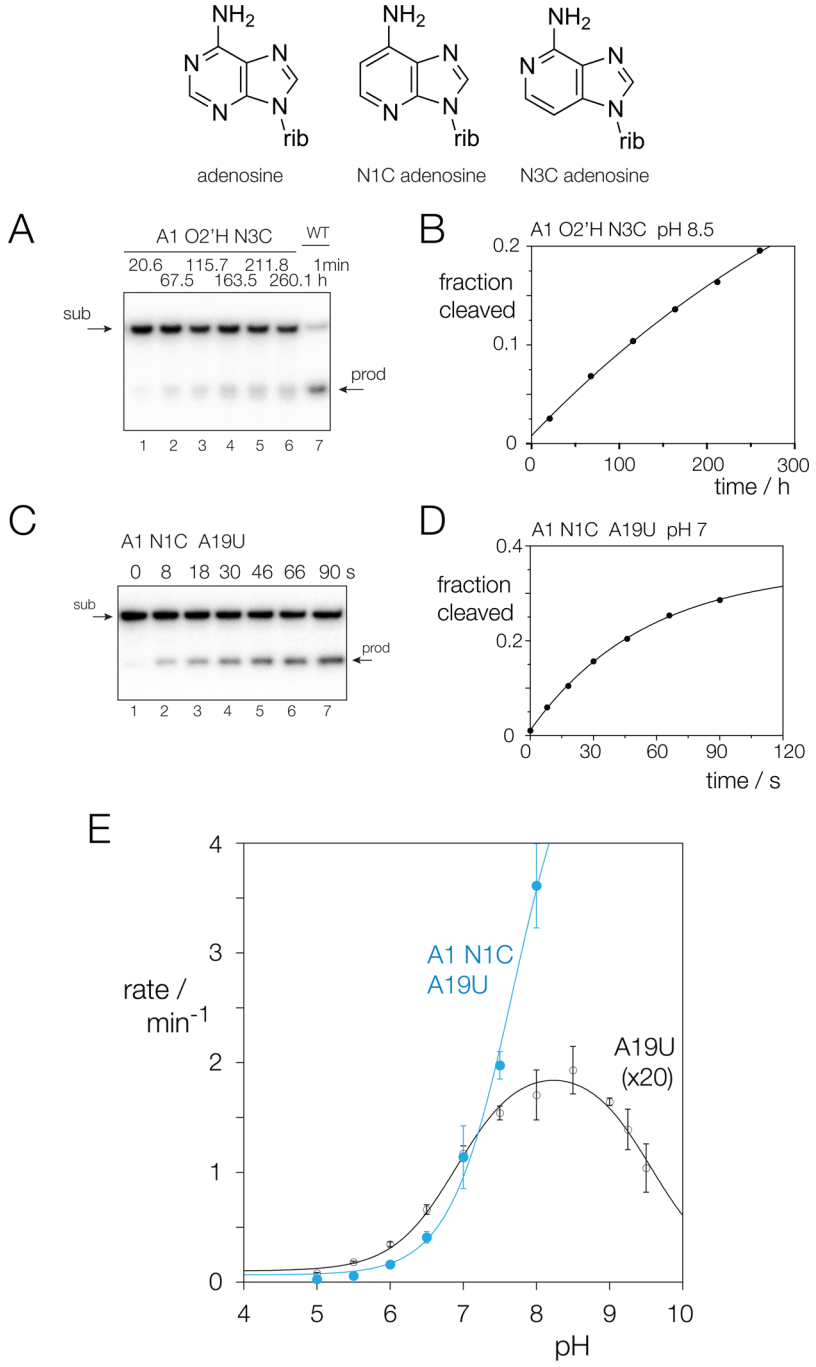

Figure 3. Effect of deaza substitution at A1 N1 and N3 atoms on twister ribozyme activity. Scheme (top) shows the chemical structures of adenosine, N1C and N3C adenosine. In these experiments the substrate strand of the two-piece ES2 ribozyme (Figure 1B) was radioactively [5′-^{32}P]-labeled. The construct was incubated in the presence of 10 mM Mg^{2+} ions, samples removed after different times and substrate (*sub*) and product (*prod*) separated by gel electrophoresis and visualized and quantified by phosphorimaging. (A) The activity of ribozyme with A1 N3C O2′H modification at pH 8.5. Incubation was performed for reaction times up to 260.1 h (tracks 1−6). A corresponding construct with an unmodified A1 was incubated for 1 min (track 7). The product appears as a doublet in the lanes arising from extended incubation times due to partial hydrolysis of the cyclic phosphate. (B) A plot of reaction progress, showing the fraction of substrate cleaved by the A1 N3C, O2′H ribozyme at pH 8.5 as a function of time (closed circles) for the data in part A. The data have been fitted to a single exponential function (line), yielding a cleavage rate of $(3.6 \pm 0.8) \times 10^{-5}$ min^{-1}. (C) The activity of ribozyme with A1 N1C A19U modifications. Incubation was performed for reaction times up to 90 s (tracks 1−7). Note that this time scale is ~10^4-fold shorter than for the corresponding incubations in part (A). (D) A plot of the fraction of substrate cleaved by the A1 N1C A19U ribozyme at pH 7.0 as a function of time (closed circles) for the data in part C. The data have been fitted to a single exponential function (line), yielding a cleavage rate of 1.1 ± 0.1 min^{-1}. (E) The experimental pH dependence of cleavage rate of the twister ribozyme with A1 N1C and A19U substitutions (blue, filled symbols). The pH dependence of cleavage rate of the A19U twister ribozyme (i.e., with adenine at position 1) is shown in black with open symbols; these data have been scaled by a factor of 20 for clarity. The data were fitted to a two-ionization model (eqs 1−3), yielding apparent pK_a values of p$K_{a,1}$ = 6.9 ± 0.1 and p$K_{a,2}$ = 9.6 ± 0.1 for the A19U ribozyme. For the A1 N1C, A19U ribozyme the pK_a values are not well determined by the data because of the monotonic increase of rate with pH. However, it can be concluded that p$K_{a,1}$ is significantly raised due to the A1 N1C substitution.

DOI: 10.1021/jacs.5b11791
J. Am. Chem. Soc. 2016, 138, 6151−6162

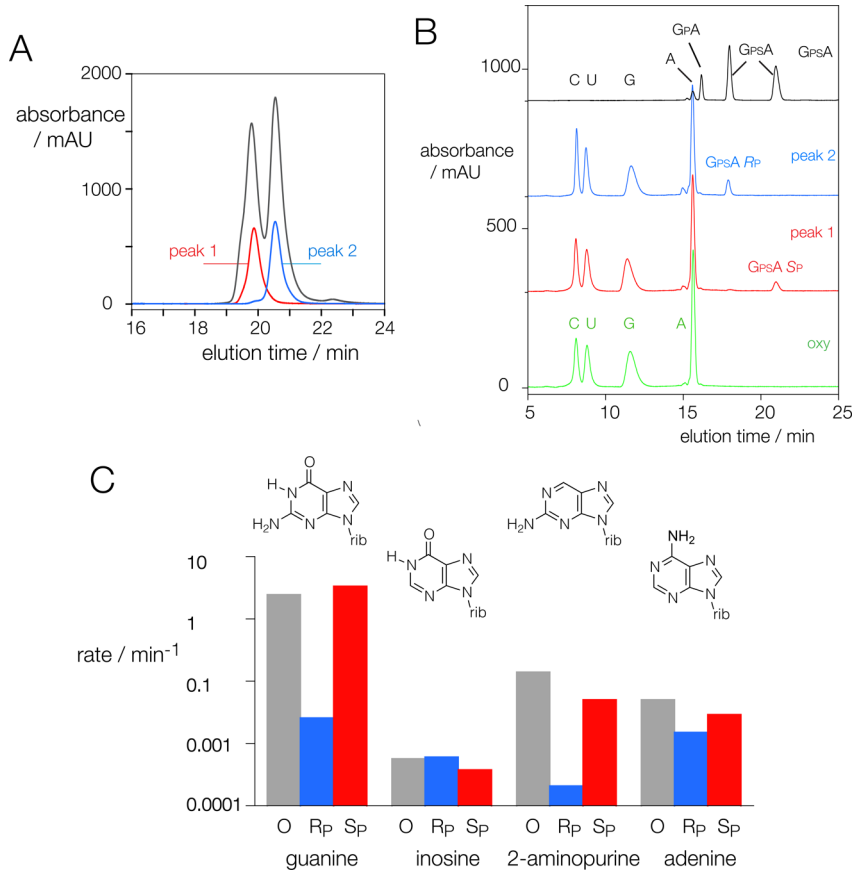

Figure 4. Activity of twister ribozyme with stereospecific phosphorothioate substitution at the scissile phosphate. (A) The substrate strand of the ES2 ribozyme was synthesized with racemic phosphorothioate substitution at the scissile phosphate, and was applied to a C18 reversed-phase column using HPLC. The elution profile (*black*) shows the separation into two peaks that were collected separately. These were individually reapplied to the column, showing elution as pure species corresponding to peak 1 (*red*) and peak 2 (*blue*) that were used in subsequent experiments. (B) The assignment of the chirality of the diastereomers separated by reversed-phase HPLC. The purified species from peaks 1 and 2 separated in part (A) were each digested with P1 nuclease to generate a relatively resistant $G_{PS}A$ dinucleotide, and separated by HPLC on a C18 reversed-phase column. A synthetic phosphorothioate-linked dinucleotide $G_{PS}A$ was also separated using the same column (*black* trace). The fast-eluting peaks are adenine and G_{PA}, followed by the $G_{PS}A$ dinucleotide migrating as two peaks, whose stereochemistry has been assigned by sensitivity to P1 and snake venom nucleases (see Figure S6). This analysis showed that the R_P diastereomer elutes at 18 min and the S_P diastereomer at 21 min. We therefore assign the stereochemistry of the substrate oligonucleotides as peak 1 (*red* trace) = S_P and peak 2 (*blue* trace) = R_P. (C) The activity of ribozymes with a stereospecific phosphorothioate modification as a function of the nucleotide present at position 33. The cleavage rates are plotted for the unmodified substrate (O) and the R_P and S_P phosphorothioates, with guanine, inosine, 2-aminopurine or adenine at position 33. The structures of these nucleosides are drawn over the corresponding data. The data for guanine and inosine were collected at pH 7.0 and the data for adenine and 2-aminopurine were collected at pH 5.5.

tions[23,24] and A is a constant specific for the particular reaction. From this it follows that the change in rate from the unmodified ribozyme (k_{unmod}) on making a modification that alters the pK_a (resulting rate k_{mod}) is given by

$$k_{mod}/k_{unmod} = 10^{\alpha \Delta pK_a} \quad (5)$$

Assuming a value of 0.5 for α, eq 5 evaluates as $10^{0.5(3.64-5.2)} = 0.166$; i.e., the rate is predicted to be 6-fold lower for the A1 N7C substituted ribozyme. Fitting the two-ionization model to the A20G and A1 N7C A20G data yielded values for k_{int} of 390 min^{-1} and 73 min^{-1} respectively, a 5.3-fold decrease. A simulated pH dependence for the A1 N7C ribozyme that takes into account the effects on $f_a \times f_b$ and k_{int} closely matches the experimental data (Figure S3). Thus, the observed increase in activity on A1 N7C substitution, together with the observed shift in pH dependence of the reaction, is consistent with the twister ribozyme utilizing concerted general acid−base catalysis involving that nucleobase. Furthermore, the magnitudes of the shift in pK_a and the decrease in k_{int} confirm that the A1 N7C substitution does not significantly perturb the ribozyme structure.

A1 N3C Virtually Abolishes Catalytic Activity. We have previously identified G33 as being responsible for the higher apparent pK_a. This together with its position in the crystal structure suggested that it was likely to act as the general base in the cleavage reaction.[8] If A1 acts as a general acid it must be doing so through the highly acidic N3 ring nitrogen as it is geometrically impossible for the more basic N1 to approach the O5′ leaving group. To test the possible role of A1 N3 we synthesized an A1 O2′H, N3C substrate. This substrate is cleaved specifically at a rate almost 10^5-fold lower (Figure 3A, B; Table 1), very close to background levels of cleavage,[5] whereas cleavage of the control A1 O2′H substrate is only 2.5-fold lower than the completely unsubstituted ribozyme at pH 7.0 (Table 1). Thus, an N3C substitution virtually abolishes catalytic activity. This observation is consistent with the hypothesis that A1 is the general acid but it remained possible

DOI: 10.1021/jacs.5b11791
J. Am. Chem. Soc. 2016, 138, 6151−6162

Table 2. Observed Cleavage Rates (min^{-1}) for the Twister Ribozyme with and without Stereospecific Sulfur Substitution at the Scissile Phosphate as a Function of the Type of Metal Cation[a]

	O		S(R_P)		S(S_P)	
	k_{obs}	±	k_{obs}	±	k_{obs}	±
10 mM Mg^{2+}	2.45	0.04	0.026 (94)	0.002	3.3 (0.74)	0.2
1 M Li^+ + 100 mM EDTA	0.090	0.007	0.0030 (30)	0.0003	0.165 (0.54)	0.009
10 mM Mg^{2+} + 10 mM Mn^{2+}	0.8	0.1	0.007 (110)	0.002	3.7 (0.23)	0.4
10 mM Mg^{2+} + 2 mM Cd^{2+}	0.43	0.06	0.046 (9.3)	0.007	5.0 (0.09)	1.0

[a]The error (±) is twice the standard deviation. The numbers in parentheses are the fold changes in rate for the phosphorothioate species compared to the oxy form studied in the same conditions.

that the loss of activity was due to a structural perturbation and that the pH dependence arose from the protonation state of N1. Therefore, we synthesized a substrate with an A1 N1C substitution. This substrate is cleaved during hybridization to the ES2 ribozyme using conditions in which the A1 N7C substrate is cleaved by the ES2 ribozyme to a minimal extent (Figure S4A, B, S5). The A1 N1C substrate survives hybridization to the A20G ribozyme but subsequent cleavage under standard conditions is too fast to measure (Figure S4C, D, S5). Therefore, we used the less-active A19U ribozyme to measure cleavage of the A1 N1C substrate. This ribozyme cleaves the A1 N1C substrate 20-fold faster than the natural sequence at pH = 7 (Figure 3C, D; Table 1). N1C-adenosine has a pK_a = 4.7[25] and therefore an A1 N1C substitution would be expected to lead to a shift in the pH dependence of the cleavage reaction in a manner similar to that observed for the A1 N7C substrate. However, since the pK_a of N1C-adenosine is intermediate between those of adenosine and N7C-adenosine, the A1 N1C substitution would be expected to have an intermediate rate of cleavage. The significantly greater activity that is observed is explained in the Discussion. We have examined the pH dependence of the cleavage of both the A1 N1C substrate and the unmodified substrate by the A19U ribozyme (Figure 3E). Cleavage of the unmodified substrate by the A19U ribozyme has a pH dependence closely similar to that of the ES2 ribozyme. The data fit the two-ionization model with pK_a values of 6.9 and 9.6, although the rate is reduced by 42-fold at pH = 7. However, the A19U A1 N1C combination resulted in a rate that increased with pH up to pH = 8.5. At pH = 9 and 9.5 the rate was too fast to measure by manual methods. The two-ionization model cannot provide a unique fit to these data, but the pH profile clearly indicates that the upper pK_a has been shifted to higher pH compared to the unmodified system. If we assume that the pK_a of ∼9.5 for G33 is retained then the significantly higher rate of reaction at pH 9.5 compared to than at pH 8.5 implies that the pK_a of A1 N1C is above pH 8.5.

Conservation of A1 and Its Importance for Catalytic Activity. An alignment of 2690 putative twister ribozyme sequences[6] reveals that A1 is one of the most highly conserved nucleotides, being present in 99.4% of the sequences. 1051 of the twister ribozymes in the alignment are found in the flatworm *Schistosoma mansoni*. Within these sequences the level of conservation of the ten most highly conserved nucleotides is lower and we have identified 16 *S. mansoni* sequences where the nucleotide at position 1 is not an A (comprising 5× C, 1× G and 10× U). By contrast, Dre-1−1 is the only example among the other 1639 twister ribozymes and this sequence lacks a P1 helix and its T1 pseudoknot can only form a single Watson−Crick base pair, suggesting that this sequence may not encode an active ribozyme.

To test the importance of A1 we transcribed in vitro the Dre-1−1 sequence and two *S. mansoni* sequences (Sma-1−827 and Sma-1−834) that exactly matched the consensus twister sequence except for a mutation at position 1 (Figure S6). No cleavage was detectable from any of the three putative ribozymes. When an A was substituted at position 1 the two ribozymes from *S. mansoni* underwent complete cleavage, showing them to be fully competent ribozymes apart from the mutation at A1. By contrast, the Dre-1−1 ribozyme exhibited only very weak activity. These observations are consistent with A1 being essential for ribozyme activity.

Stereospecific Effects of Phosphorothioate Substitution on Cleavage Rates. To identify additional functionally important interactions of the active ribozyme we sought to characterize the origin of the previously reported phosphorothioate effect.[6,18] A substrate with a phosphorothioate substitution at the scissile phosphate was synthesized and the diastereomers were separated by reversed-phase HPLC as peak 1 and peak 2 (Figure 4A). In order to identify the R_P and S_P diastereomers, the unmodified substrate and the two resolved phosphorothioate diastereomers were individually digested with nuclease P1 in the presence of a 5′ phosphatase (Figure 4B). While the oxy substrate was hydrolyzed down to the four nucleosides, both phosphorothioate forms resulted in an extra peak corresponding to the $G_{PS}A$ dinucleotide that is relatively resistant to nuclease digestion. The oligonucleotide peak 1 (from the separation in Figure 4A) gave a $G_{PS}A$ dinucleotide eluting at 21 min, while the corresponding dinucleotide generated from peak 2 eluted at 18 min. These have been unambiguously assigned by nuclease digestion of a synthetic $G_{PS}A$ dinucleotide (Figure S7) to be S_P and R_P diastereomers, respectively. Thus, the substrate with the S_P diastereomer eluted first whereas it is normally the R_P diastereomer that elutes first.[26]

The purified diastereomers of the substrate were incubated with ribozyme in the presence of 10 mM $MgCl_2$ at pH 7.0. The S_P diastereomer was cleaved at 3.3 min^{-1}, a rate slightly higher than that of the unmodified substrate, while the R_P diastereomer was cleaved at a rate of 0.026 min^{-1} (Figure 4C, Table 2). This 120-fold stereospecific effect compares to the 50-fold effect previously reported,[6] corresponding to a stabilization of the transition state by 12 kJ mol^{-1}. A stereospecific effect of similar magnitude was observed when the reactions were performed in 1 M LiCl in the absence of divalent cations (Table 2). This observation suggests that the stereospecific effect does not arise through a specific interaction between magnesium ions and the scissile phosphate.

In our crystal structure of the twister ribozyme[8] G33 N2 donates a hydrogen bond to the *pro*R nonbridging oxygen of the scissile phosphate (Figure 1C). The importance of this exocyclic amine is demonstrated by the 500-fold reduction in

DOI: 10.1021/jacs.5b11791
J. Am. Chem. Soc. 2016, 138, 6151−6162

activity observed when inosine, which lacks the N2, is substituted for G33.[8] Therefore, we investigated the hypothesis that the loss of the hydrogen bond between G33 and the *pro*R nonbridging oxygen is the source of the stereospecific phosphorothioate effect. A nucleobase substitution that is unable to hydrogen bond to the scissile phosphate would not be expected to exhibit a stereospecific effect, and this is observed for the G33I substitution, where there is only a 2-fold difference in activity between the R_P and S_P diastereomers (Figure 4C). Further support for the hypothesis is provided by comparison of two further substitutions. 2-aminopurine, which has an N2 exocyclic amine, exhibits a strong stereospecific effect, whereas adenine, which lacks the exocyclic amine, has a significantly reduced effect (Figure 4C). We conclude that the hydrogen bond donated by N2 of G33 to the *pro*R nonbridging oxygen is responsible for significant stabilization of the transition state (process 2).

The data above provide strong evidence for an interaction between G33 N2 and the *pro*R nonbridging oxygen of the scissile phosphate. In addition we sought to test the possibility of an interaction of either nonbridging oxygen with a metal ion in the transition state of the cleavage reaction. We compared the rate of cleavage of the substrate strand with the normal oxy substrate and the two resolved phosphorothioate-substituted forms in the presence of two thiophilic metal ions, manganese and cadmium, in addition to the usual Mg^{2+} ions (Table 2). In the presence of 10 mM Mn^{2+} ions cleavage rates for the oxy and R_P phosphorothioate substrates were reduced ~3-fold while the rate for the S_P phosphorothioate was unchanged. Somewhat larger effects were observed for Cd^{2+} ions. Inhibition of cleavage of the oxy substrate was twice that obtained with Mn^{2+} ions. An apparent restoration of activity was observed for both phosphorothioate diastereomers, but this was mostly due to the loss of activity of the oxy form rather than a stimulation of activity of the phosphorothioates. These results reinforce the importance of the G33 N2 bond to the *pro*R nonbridging oxygen as the R_P phosphorothioate substrate is consistently cleaved 2 orders of magnitude slower than the S_P phosphorothioate substrate.

These results are very similar to the data of Kosutic et al.[18] It is difficult to assess rates because of the qualitative nature of their data, but they too observe an inhibition of cleavage of the oxy form and an enhancement of cleavage of both phosphorothioate diastereomers by Cd^{2+} ions, and the magnitude of the changes in rate appear to be similar. The small magnitudes of the effects and the fact that both diastereomers respond similarly to Cd^{2+} ions leads us to conclude that the evidence to support a direct interaction with a metal ion in the transition state is not strong. The major effect of phosphorothioate substitution at the scissile phosphate arises from the interaction with G33 N2.

DISCUSSION

Atomic mutagenesis of the adenine nucleobase at position 1 of the twister ribozyme has established that the pH dependence of the cleavage reaction arises in part from the protonation state of the N3 ring nitrogen of that adenine. The twister ribozyme exhibits bell-shaped pH dependence with apparent pK_a values of 6.9 and 9.5. We have previously identified G33 as being responsible for the upper pK_a and here we have shown that A1 is responsible for the lower pK_a. The change in the pH dependence and magnitude of activity for substitutions at G33[8] and A1 (this work) are readily explained by a mechanism of concerted general-acid-base catalysis, and it is difficult to envisage an alternative mechanism consistent with all the data, especially the enhanced activity of an A1 N7C substitution. A1 N3 is only 4.5 Å from the O5′ leaving group in the crystal structure and is thus well placed to act as a general acid (Figure 1C), in which case G33 must act as a general base as we have previously proposed.[8] The alternative of A1 acting as general base and G33 as general acid is structurally implausible.

The finding that the general acid is the adenine N3 is somewhat unexpected as N3 is the least basic of the three ring nitrogen atoms. Other ribozymes known to utilize adenine do so through the more basic N1.[15,27−29] The basicity of the nitrogen atoms of adenosine follow the order N3 < N7 < N1, with microscopic pK_a values of 1.5, 2.15, and 3.63.[20] It follows that the distribution of tautomers for singly protonated adenosine are N3 0.7%, N7 3.2% and N1 96.1% (Figure 5A). Assuming similar proportions apply to the ribozyme, the N3 will be only weakly protonated, even at pH 5.0 where almost all

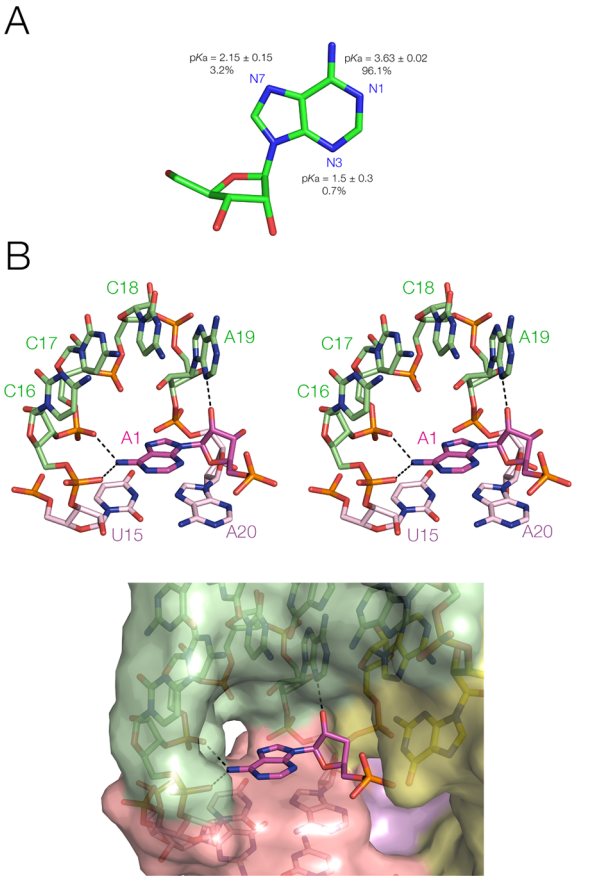

Figure 5. Structure of the A1-binding pocket. (A) The microscopic pK_a values of the ring nitrogen atoms N1, N3 and N7 of adenine, and calculated fractional protonation.[20] (B) The A1-binding pocket in the crystal structure of the *O. sativa* twister ribozyme.[8] A1 is surrounded by the nucleotides of L4 that include the T1 interaction (C16 to A19) closed by the basepair between U15 and A20. These images are rotated 180° vertically compared to the view of the ribozyme in Figure 1, so that the T1 nucleotides (green) are at the top, and the P4 stem (red) is at the bottom. Upper: Parallel-eye stereoscopic view of the of the binding pocket with the nucleotides shown in stick form, with key hydrogen bonds indicated by broken lines. Lower: A similar view with a surface on the surrounding nucleotides to highlight the binding pocket. Additional coloring shows the P2 helix (yellow) and the T2 tertiary interaction (violet).

DOI: 10.1021/jacs.5b11791
J. Am. Chem. Soc. 2016, 138, 6151−6162

adenines at position 1 will carry a charge of +1. However, the low fraction in the active $N3H^+$ state will be offset to some extent by the greater reactivity of the acid. The simple formulation used in eq 1 assumes a single site of protonation, which is appropriate if catalysis occurs through N1. In this case the equation requires a correction for the fractional protonation of N3:

$$k_{obs} = k_{max} \times f_{N3H} \times f_a \times f_b \quad (6)$$

where f_{N3H} is the fraction of protonation occurring at N3. Nevertheless, the comparison between adenine and N7C-adenine is valid assuming the basicities of N1 and N3 are raised to a similar extent and f_{N3H} is approximately constant over the observable pH range, in which case only the product $f_a \times f_b$ will determine the pH dependence for each nucleotide. However, f_{N3H} will change as the pH decreases toward the second macroscopic pK_a of these nucleobases, which lies 5 pH units below the first macroscopic pK_a.[20] It is also possible that titration of another species close to A1 such as A20 may influence f_{N3H}. Changes in f_{N3H} may explain the deviations from the simple model used to fit the data that are apparent at low pH in Figures S3 and S5.

An increase in the fractional protonation of N3 is the likely explanation for the significantly higher activity of an A1 N1C substitution. The data in Figure 3E suggests that the A1 N1C has a pK_a > 8.5. Therefore, A1 N1C and A1 N7C will have virtually identical $f_a \times f_b$ at pH 7 and A1 N7C will have the higher intrinsic activity. Yet the observed activity of A1 N7C A20G is 0.28 min^{-1} (Table 1) while that of A1 N1C A20G is >8 min^{-1} (Figure S4C,D), an increase of at least 30-fold. However, in the case of N1C adenosine N3 is more basic than N7, and $N3H^+$ is the predominant tautomer (f_{N3H} > 0.5).[30] This difference in f_{N3H} is sufficient to account for the much higher activity of A1 N1C A20G.

The apparent pK_a = 6.9 for A1 compares to the value of 3.64 for adenosine, indicating a strong environmental influence. A1 is located in a pocket created by the interaction of loops L1 and L4, stacked on the final base pair of P4 and making three hydrogen bonds to the L4 strand of T1 (Figure 5B). The 2′-*endo* sugar pucker and the *syn* conformation position N3 close to the O5′ leaving group so that it can function as a general acid. Of particular significance, A1 N6 donates hydrogen bonds to the nonbridging oxygen atoms of two successive phosphates (C16 and C17). Hence the six-membered ring of A1 lies between three phosphate groups, and proximity to negatively charged anions would be expected to stabilize the active, protonated nucleobase, resulting in the raised pK_a. The importance of the N6 of A1 is emphasized by the much lower activity of an A1G substitution. Like adenine, guanine has an N3 and could act as an effective general acid. However, the loss of the two hydrogen bonds donated by N6 of adenine will affect the positioning of the nucleobase and presumably also result in a less substantial increase in microscopic pK_a for the N3. The same arguments can explain the loss of activity on substitution by 2-aminopurine.[18] In principle the extent of protonation at N3 would be increased if either N1 or N7 were to accept a hydrogen bond, thereby reducing their microscopic pK_a. This does not appear to be the case for the twister ribozyme. N1 of A1 is in a relatively open location in the crystal and there is nothing close by that could donate a proton (Figures 1C and 5B). N7 sits deep in the A1 binding pocket, the nearest atoms being nonbridging phosphate oxygen atoms of T1 (Figure 5B). Again, there are no proton donors in the vicinity. Nevertheless, we hypothesize that the local environment of A1 could alter the relative basicity of the three ring nitrogen atoms such that the fractional protonation of A1 N3 is greater than that observed for adenosine.

Two other laboratories have recently proposed alternative catalytic strategies based upon structures of different forms of the twister ribozyme.[16−18] In most aspects there is excellent agreement between the structures. The global folds are the same, as is the positioning of A1 in its pocket stacked on the end of P4, and in each case G33 is in close proximity to the scissile phosphate. However, the structures differ in the location of U-1 and the interactions made with the nonbridging oxygen atoms of the scissile phosphate. Eiler et al. solved two structures but U-1 could only be modeled in the lower resolution 4.1 Å structure, where it has a non in-line position similar to U-1 in our structure. The N6 of A34 is close to the scissile phosphate and it was proposed that this provided transition state stabilization through bonding to the *pro*S nonbridging oxygen. However, this proposal is not supported by our mechanistic studies. An A34G substitution results in only a minor decrease in activity,[8] and the *Sp* phosphorothioate has normal levels of activity, yet both modifications would disrupt the proposed hydrogen bond.

The structure of the *env*22 twister ribozyme solved by Ren et al.[17] has a near in-line orientation and a Mg^{2+} ion bound to the *pro*S nonbridging oxygen of the scissile phosphate as an inner-sphere complex. The P1 helix has adopted a different structure with two uridine residues (positions −2 and −5 in our new numbering scheme) forming base triples with nucleotides in T1 instead of pairing with their complementary nucleotides in P1. This alternative P1 structure is not supported by the alignment of twister ribozymes, in which the standard base pairing of P1 is conserved but the sequence is not.[6] This alignment very successfully predicted the secondary structure, including the two pseudoknots, together with the nucleobases making important noncanonical interactions. Nor is it consistent with the structure of the ES2 ribozyme used in our mechanistic studies that has a 10 base pair P1 helix and a sequence that cannot form the base triples. Crucially, it is not possible for U-1 to adopt the in-line orientation of the *env*22 structure if P1 is fully base paired (Figure S8). Effective catalysis requires more than an in-line trajectory.[5,31] In the *env*22 structure there is nothing nearby that could activate the nucleophile (G33 N1 donates a hydrogen bond to the *pro*R oxygen of the scissile phosphate), and while the bound Mg^{2+} ion would help stabilize the transition state it would also prevent the rotation required to bring the O5′ into proximity with N3 of A1, and there is no alternative in place that could serve to protonate the leaving group. Furthermore, the U to C mutation intended to test the integrity of the Mg^{2+} ion binding site had a negligible effect on activity.[17] Thus, it seems that the in-line orientation was adopted adventitiously as a result of the misfolding of P1 and stabilized by crystal contacts and Mg^{2+} ion binding, and that neither the in-line orientation nor the bound Mg^{2+} ion are relevant to the structure adopted by the active ribozyme.

While there are considerable reasons to doubt the relevance of the Mg^{2+} ion binding site observed in the *env*22 structure, this does not mean that Mg^{2+} ions have no role in twister ribozyme catalysis. Comparison of the activity in divalent and monovalent ions[6,8] (this work) indicates that Mg ions (and some other divalent ions) do enhance activity. Possible mechanisms include stabilization of the folded structure by binding at one or more of the sites observed in the crystal

DOI: 10.1021/jacs.5b11791
J. Am. Chem. Soc. 2016, 138, 6151−6162

structures,[8,17] nonspecific electrostatic stabilization of the transition state, and specific binding of a Mg^{2+} ion to the scissile phosphate. Our data demonstrate that the 100-fold slower rate of cleavage of the R_P phosphorothioate substrate is due to the loss of a hydrogen bond donated by G33 N2. However, the increased cleavage rate of both R_P and S_P phosphorothioate substrates in the presence of Cd^{2+} ions[18] (this work), leaves open the possibility of a specific interaction between a Mg^{2+} ion and the scissile phosphate.

We have previously shown that a simple, unhindered rotation of the U-1 from its position in the crystal structure such that the uridine stacks underneath G33 could produce the necessary in-line orientation.[8] A model of the active site incorporating this relocation of nucleotide −1 into the T1 major groove is fully consistent with all our experimental observations, and provides a consistent description of the catalytic mechanism of the twister ribozyme in terms of the four identified factors leading to rate enhancement (Figure 6). It brings the O2′ nucleophile into position to attack the scissile phosphorus atom in-line (process 1). G33 N2 makes an interaction with the *pro*R nonbridging O of the scissile phosphate, positioning the nucleobase and providing a significant stabilization of the transition state (process 2). G33 N1 is juxtaposed with the O2′, well positioned to remove its proton and thus greatly increase its nucleophilicity (process 3). General base catalysis is complemented by protonation of the leaving oxyanion by a general acid (process 4), and our data are fully consistent with A1 in this role. Recent molecular dynamics simulations agree with our model, finding that the twister ribozyme attains an in-line orientation with U-1 stacked under G33 and with G33 N1 and A1 N3 poised to participate in general acid−base catalysis.[9]

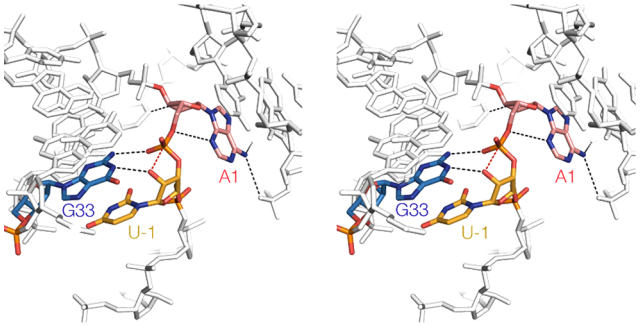

Figure 6. Proposed catalytic mechanism for cleavage by the twister ribozyme. Parallel-eye stereoscopic view of the active center of the twister ribozyme, remodeled to bring U-1 below G33 in the major groove of the T1 helix, and with the addition of a 2′-hydroxyl group at U-1 (i.e., the reaction nucleophile). This view can be compared with the unmodified crystal structure shown in Figure 1C. In the remodeled structure the U-1 O2′ is now well aligned for in-line attack on the adjacent phosphorus (broken red line), and is close to G33 N1. The exocyclic N2 of G33 is hydrogen bonded to the *pro*R nonbridging oxygen of the scissile phosphate. The A1 nucleobase within its binding pocket (Figure 5B) directs its N3 toward the O5′ of the scissile phosphate. Thus, G33 is well positioned to act as the general base removing a proton from the O2′ of the nucleophile, while A1 N3 is similarly well positioned to protonate the O5′ of the oxyanion leaving group.

There are two completely novel aspects to the role of A1. First, it is immediately 3′ to the scissile phosphate, and second, the proton is transferred from N3 rather than the more basic N1. This is achieved by locating A1 in a highly specific binding pocket, where it hydrogen bonds to the nonbridging oxygen atoms of successive anionic phosphate groups of T1, raising its macroscopic pK_a and thus increasing the population of active ribozyme. The position of A1 in the pocket is also important in generating the splayed-apart conformation of the nucleotides on either side of the scissile phosphate, thereby facilitating an in-line trajectory. Evidently the entire fold of the ribozyme has evolved to create this pocket. The way the twister ribozyme holds A1 and activates it to act as a general acid is unique, and a demonstration of the remarkable versatility of RNA catalysis.

EXPERIMENTAL SECTION

RNA Synthesis. Oligonucleotides were synthesized using *t*-BDMS phosphoramidite chemistry[32] implemented on an Applied Biosystems 394 synthesizer.[33] RNA was synthesized using UltraMILD ribonucleotide phosphoramidites with 2′-*O*-*tert*-butyldimethyl-silyl (*t*-BDMS) protection[34,35] (Link Technologies). Phosphoramidite for incorporation of N7C adenine was from ChemGenes and for N3C O2′H adenine was from Glen Research. The N1C phosphoramidite was synthesized (see below). RNA with a sulfur substitution was synthesized in the same manner except that the iodine oxidation step of the synthesis cycle was replaced with reaction with 3*H*-1,2-benzodithiol-3-one-1,1-dioxide (Beaucage reagent) to generate the phosphorothioate linkage.[36] Oligoribonucleotides were deprotected in 1:1 ammonia/methylamine at 60 °C for 20 min and evaporated to dryness. They were redissolved in 115 μL of anhydrous DMSO, 60 μL triethylamine and 75 μL triethylamine trihydrofluoride (Aldrich) and incubated at 65 °C for 2.5 h to remove *t*-BDMS groups, and normally recovered by butanol precipitation. However, the A1 N1C substrate was passed through a NAP 10 column (GE Life Sciences) and recovered by ethanol precipitation. Dinucleotides were purified on a disposable Sep-Pak C18 column according to the manufacturer's instructions, evaporated to dryness, redissolved in water and used without further purification. Transcribed RNA was synthesized using T7 RNA polymerase[37] and templates made by recursive PCR from synthetic DNA oligonucleotides.

RNA was purified by electrophoresis in 14% polyacrylamide gels containing 90 mM Tris·borate (pH 8.3), 10 mM EDTA (TBE buffer) and 7 M urea, visualized by UV shadowing, and excised gel slices were crushed and soaked overnight in 10 mM Tris-Cl (pH 8.0), 300 mM Na acetate, 1 mM EDTA. Following removal of polyacrylamide fragments by filtration, RNA was recovered by ethanol precipitation, redissolved in water and stored at −20 °C.

Synthesis of N1C Adenine Phosphoramidite. The general synthesis of the adenosine analogue N1C adenosine (**1**) was done according to the procedures of Petrelli and co-workers[38] and Geroni and co-workers.[39] The synthesis of the N1C phosphoramidite from (**1**) required modification of routine procedures and is detailed in Supplemental Note 1.

Mass Spectroscopy of Oligonucleotides. Successful synthesis and deprotection of the A1 N1C substrate was verified by mass spectroscopy (Figure S8). ESI mass spectra were recorded on an HTC Esquire mass spectrometer (Bruker Daltonic) in combination with an 1100 Series HPLC system (Agilent Technologies) using 10 mM triethylamine/100 mM hexafluoroisopropanol as buffer A and acetonitrile as eluent (buffer B). RNA oligonucleotides were desalted prior to MS using Zip-tip C18 pipet tips (Millipore).

Purification and Characterization of Phosphorothioate-Modified Oligonucleotides. Following purification by gel electrophoresis, the R_P and S_P diastereomers of the phosphorothioate modified substrate oligonucleotide were separated by reversed-phase HPLC using a semipreparative C18 column (ACE 5 C18-AR, 250 × 4.6 mm) and a photodiode array absorbance detector. The elution conditions were 2−8% acetonitrile (3 min) followed by 8−12% acetonitrile (20 min) in 0.1 M triethylammonium acetate at a flow rate of 0.5 mL/min. Peak fractions of the partially resolved diastereomers were subjected to a second run using the same conditions (Figure 4A) to increase their purity. The leading edge of peak 1 and the trailing

DOI: 10.1021/jacs.5b11791
J. Am. Chem. Soc. 2016, 138, 6151−6162

edge of peak 2 were collected separately and used for mechanistic studies.

To assign the R_P and S_P diastereomers we first synthesized and characterized a $G_{PS}A$ dinucleotide. The diastereomers of $G_{PS}A$ were well resolved by reversed-phase HPLC using the column and solvent system described above and an gradient of 2−7% acetonitrile (2.5 min) followed by 7−11% acetonitrile (20 min). Nuclease P_1 from *Penicillium citrinum* (Sigma-Aldrich), which preferentially cleaves S_P phosphorothioates,[40] and Phosphodiesterase I from *Crotalus atrox* (Type IV, Sigma-Aldrich), which preferentially cleaves R_P phosphorothioates,[41] were used to assign the diastereomers. Both enzymes cleave phosphodiester linkages significantly faster than phosphorothioate linkages. 8.8 nmol diastereomer was incubated at 37 °C for 4 h with either 4 μg nuclease P_1 (0.75 units) in 30 μL 30 mM sodium acetate (pH 5.3) supplemented with 0.1 mM $ZnCl_2$, or 30 μg phosphodiesterase I (6×10^{-4} units) in 30 μL 50 mM TrisCl (pH 7.5), 10 mM $MgCl_2$ and 0.1 mM EDTA. 80 units Antarctic Phosphatase (New England Biolabs) was present in the reaction mixtures to ensure that the digestion products were dephosphorylated. The resulting mixture of nucleosides and $G_{PS}A$ dinucleotide was passed through a 30K centrifugal filter (Amicon) to remove the enzymes and separated by reversed-phase HPLC as described above. The changes in the relative amounts of the diastereomers following digestion demonstrated that the R_P diastereomer eluted prior to the S_P diastereomer (Figure S7).

Oligonucleotides were digested by nuclease P_1 and separated by reversed-phase HPLC in an identical fashion except that 500 pmol oligonucleotide was incubated at 37 °C for 30 min with 20 ng nuclease P_1 (0.004 units) and 80 units Antarctic Phosphatase to achieve complete digestion of the phosphodiester linkages while leaving the phosphorothioate linkages substantially intact. The time of elution of the GpsA dinculeotide permitted the assignment of peak 1 as S_P and peak 2 as R_P (Figure 4B). All peaks were unambiguously identified by their UV spectra.

Analysis of Ribozyme Kinetics. The ES2 twister ribozyme used for kinetic analysis is derived from the Type P3 env-9 environmental sequence.[6,8] ES2 is assembled from two oligonucleotides (Figure 1B), termed ribozyme and substrate:

Ribozyme (50 nt): GGCAAUAAAGCGGUUACAAGCCCG-CAAAAAUAGCAGAGUAUGUCGCUGGU.

Substrate (28 nt): ACCAGCGGCAGAAUGCAGCUUUAU-UGCC.

These were made by transcription and chemical synthesis respectively, incorporating modified nucleosides where necessary. For synthetic convenience an additional dT nucleotide was added to the 3′ end of the substrate with an A1 N1C modification.

Cleavage kinetics were studied under single-turnover conditions. Normally, ribozyme and radioactively [5′-^{32}P]-labeled substrate were annealed in 50 mM NaCl, 0.1 mM EDTA (pH 7.0) by heating to 80 °C and allowing to cool to room temperature over 2 h. However, these conditions resulted in cleavage of A1 N7C substrate when annealed to the unmodified ribozyme strand, and A1 N1C substrate when incubated with any ribozyme strand. In these cases ribozyme and substrate were annealed by rapid cooling (0.2 °C per second) from 80 to 25 °C in a thermal cycler.

Aliquots of annealed ES2 were equilibrated to 25 °C and the reaction initiated by adding an equal volume of equilibrated 2x reaction buffer. The final reaction contained 1 μM ribozyme and 10 nM substrate. Standard reaction conditions were 25 mM HEPES (pH 7.0), 10 mM $MgCl_2$, 100 mM NaCl, 0.05 mM EDTA. These conditions were supplemented with either 10 mM $MnCl_2$ or 2 mM $CdCl_2$ as required for the study of the phosphorothioate substitutions. Activity in monovalent ions was investigated using 25 mM HEPES (pH 7.0), 1.0 M LiCl, 100 mM EDTA, the latter to sequester any divalent ions that may be present. For the study of the pH dependence of rates, standard conditions were used except that 25 mM of the following buffers were used to achieve the desired pH: MES, pH 4.75−6.75; HEPES, pH 7.0−7.5; TAPS, pH 8.0−9.0; CHES, pH 9.25−9.5. Slow reactions requiring long incubations (up to 260 h) were carried out under mineral oil to prevent evaporation. Two μL aliquots were removed at intervals and the reaction terminated by addition to 13 μL of a mixture containing 95% (v/v) formamide, 50 mM EDTA and electrophoresis dyes. Substrate and product were separated by electrophoresis in 20% polyacrylamide gels containing 7 M urea and quantified by phosphorimaging. Progress curves were fitted by nonlinear regression analysis to single exponential functions using Kalaidagraph (Abelbeck Software).

Modeling the Active Site of the Twister Ribozyme. To generate a model of the active site with an in-line trajectory and that is consistent with the biochemical data, a 2′ hydroxyl was added to the dU-1 nucleotide in the twister crystal structure and the nucleotide was rotated toward A34 about an axis passing through the phosphorus atoms of U-1 and A1 without the breaking of any covalent bonds. The rotation was terminated at the point where the O2′−P-O5′ angle was greatest. After rotation, the uracil of U-1 was rotated so that it stacked with the guanine of G33. Residues 33 and 34 were then moved approximately 1 Å in order to increase the separation between G33 and U-1 to a distance suitable for hydrogen bonds. Finally, the model was energy minimized using GROMACS 5.0 (M.J. Abraham, D. van der Spoel, E. Lindahl, B. Hess, and the GROMACS development team, GROMACS User Manual version 5.0.4, www.gromacs.org (2014)).

■ ASSOCIATED CONTENT

Supporting Information

The Supporting Information is available free of charge on the ACS Publications website at DOI: 10.1021/jacs.5b11791.

Nine figures and two tables. (PDF)

■ AUTHOR INFORMATION

Corresponding Author

*d.m.j.lilley@dundee.ac.uk

Notes

The authors declare no competing financial interest.

■ ACKNOWLEDGMENTS

We thank Dr. Darrin York and Colin Gaines (Rutgers) for discussion and data sharing, and Saira Ashraf for expert synthesis of RNA. The work was funded by Cancer Research UK (Program grant A11722 to DMJL) and Fonds der Chemischen Industrie (Liebig-fellowship LI 191/08 to SKS).

■ REFERENCES

(1) Nissen, P.; Hansen, J.; Ban, N.; Moore, P. B.; Steitz, T. A. *Science* **2000**, *289*, 920.

(2) Fica, S. M.; Tuttle, N.; Novak, T.; Li, N. S.; Lu, J.; Koodathingal, P.; Dai, Q.; Staley, J. P.; Piccirilli, J. A. *Nature* **2013**, *503*, 229.

(3) Webb, C. H.; Riccitelli, N. J.; Ruminski, D. J.; Luptak, A. *Science* **2009**, *326*, 953.

(4) Seehafer, C.; Kalweit, A.; Steger, G.; Graf, S.; Hammann, C. *RNA* **2011**, *17*, 21.

(5) Soukup, G. A.; Breaker, R. R. *RNA* **1999**, *5*, 1308.

(6) Roth, A.; Weinberg, Z.; Chen, A. G.; Kim, P. B.; Ames, T. D.; Breaker, R. R. *Nat. Chem. Biol.* **2014**, *10*, 56.

(7) Weinberg, Z.; Kim, P. B.; Chen, T. H.; Li, S.; Harris, K. A.; Lunse, C. E.; Breaker, R. R. *Nat. Chem. Biol.* **2015**, *11*, 606.

(8) Liu, Y.; Wilson, T. J.; McPhee, S. A.; Lilley, D. M. J. *Nat. Chem. Biol.* **2014**, *10*, 739.

(9) Gaines, C. S.; York, D. M. *J. Am. Chem. Soc.* **2016**, *138*, 3058.

(10) Pinard, R.; Hampel, K. J.; Heckman, J. E.; Lambert, D.; Chan, P. A.; Major, F.; Burke, J. M. *EMBO J.* **2001**, *20*, 6434.

(11) Wilson, T. J.; Ouellet, J.; Zhao, Z. Y.; Harusawa, S.; Araki, L.; Kurihara, T.; Lilley, D. M. J. *RNA* **2006**, *12*, 980.

(12) Kath-Schorr, S.; Wilson, T. J.; Li, N. S.; Lu, J.; Piccirilli, J. A.; Lilley, D. M. *J. Am. Chem. Soc.* **2012**, *134*, 16717.

DOI: 10.1021/jacs.5b11791
J. Am. Chem. Soc. 2016, 138, 6151−6162

(13) Wilson, T. J.; Li, N.-S.; Lu, J.; Frederiksen, J. K.; Piccirilli, J. A.; Lilley, D. M. J. *Proc. Natl. Acad. Sci. U. S. A.* **2010**, *107*, 11751.
(14) Wilson, T. J.; McLeod, A. C.; Lilley, D. M. J. *EMBO J.* **2007**, *26*, 2489.
(15) Suslov, N. B.; DasGupta, S.; Huang, H.; Fuller, J. R.; Lilley, D. M. J.; Rice, P. A.; Piccirilli, J. A. *Nat. Chem. Biol.* **2015**, *11*, 840.
(16) Eiler, D.; Wang, J.; Steitz, T. A. *Proc. Natl. Acad. Sci. U. S. A.* **2014**, *111*, 13028.
(17) Ren, A.; Kosutic, M.; Rajashankar, K. R.; Frener, M.; Santner, T.; Westhof, E.; Micura, R.; Patel, D. J. *Nat. Commun.* **2014**, *5*, 5534.
(18) Kosutic, M.; Neuner, S.; Ren, A.; Flur, S.; Wunderlich, C.; Mairhofer, E.; Vusurovic, N.; Seikowski, J.; Breuker, K.; Hobartner, C.; Patel, D. J.; Kreutz, C.; Micura, R. *Angew. Chem., Int. Ed.* **2015**, *54*, 15128.
(19) Ravindranathan, S.; Butcher, S. E.; Feigon, J. *Biochemistry* **2000**, *39*, 16026.
(20) Kapinos, L. E.; Operschall, B. P.; Larsen, E.; Sigel, H. *Chem. - Eur. J.* **2011**, *17*, 8156.
(21) Fasman, G. D. *Handbook of Biochemistry and Molecular Biology*, CRC Press: Cleveland, OH, 1975.
(22) Bevilacqua, P. C. *Biochemistry* **2003**, *42*, 2259.
(23) Nakano, S.; Proctor, D. J.; Bevilacqua, P. C. *Biochemistry* **2001**, *40*, 12022.
(24) Shih, I. H.; Been, M. D. *Proc. Natl. Acad. Sci. U. S. A.* **2001**, *98*, 1489.
(25) Itoh, T.; Kitano, S.; Mizuno, Y. *J. Heterocycl. Chem.* **1972**, *9*, 465.
(26) Frederiksen, J. K.; Piccirilli, J. A. *Methods Enzymol.* **2009**, *468*, 289.
(27) Rupert, P. B.; Massey, A. P.; Sigurdsson, S. T.; Ferré-D'Amaré, A. R. *Science* **2002**, *298*, 1421.
(28) MacElrevey, C.; Salter, J. D.; Krucinska, J.; Wedekind, J. E. *RNA* **2008**, *14*, 1600.
(29) Spitale, R. C.; Volpini, R.; Heller, M. G.; Krucinska, J.; Cristalli, G.; Wedekind, J. E. *J. Am. Chem. Soc.* **2009**, *131*, 6093.
(30) Seela, F.; Debelak, H.; Usman, N.; Burgin, A.; Beigelman, L. *Nucleic Acids Res.* **1998**, *26*, 1010.
(31) Emilsson, G. M.; Nakamura, S.; Roth, A.; Breaker, R. R. *RNA* **2003**, *9*, 907.
(32) Beaucage, S. L.; Caruthers, M. H. *Tetrahedron Lett.* **1981**, *22*, 1859.
(33) Wilson, T. J.; Zhao, Z.-Y.; Maxwell, K.; Kontogiannis, L.; Lilley, D. M. J. *Biochemistry* **2001**, *40*, 2291.
(34) Hakimelahi, G. H.; Proba, Z. A.; Ogilvie, K. K. *Tetrahedron Lett.* **1981**, *22*, 5243.
(35) Perreault, J.-P.; Wu, T.; Cousineau, B.; Ogilvie, K. K.; Cedergren, R. *Nature* **1990**, *344*, 565.
(36) Iyer, R. P.; Egan, W.; Regan, J. B.; Beaucage, S. L. *J. Am. Chem. Soc.* **1990**, *112*, 1253.
(37) Milligan, J. F.; Groebe, D. R.; Witherall, G. W.; Uhlenbeck, O. C. *Nucleic Acids Res.* **1987**, *15*, 8783.
(38) Antonini, I.; Cristalli, G.; Franchetti, P.; Grifantini, M.; Martelli, S.; Petrelli, F. *J. Pharm. Sci.* **1984**, *73*, 366.
(39) Cristalli, G.; Franchetti, P.; Grifantini, M.; Vittori, S.; Bordoni, T.; Geroni, C. *J. Med. Chem.* **1987**, *30*, 1686.
(40) Potter, B. V.; Connolly, B. A.; Eckstein, F. *Biochemistry* **1983**, *22*, 1369.
(41) Bryant, F. R.; Benkovic, S. J. *Biochemistry* **1979**, *18*, 2825.

DOI: 10.1021/jacs.5b11791
J. Am. Chem. Soc. 2016, 138, 6151−6162